



Modeling, identification and feedforward control of multivariable hysteresis by combining Bouc-Wen equations and the inverse multiplicative structure.

Didace Habineza, Micky Rakotondrabe, Yann Le Gorrec

► To cite this version:

Didace Habineza, Micky Rakotondrabe, Yann Le Gorrec. Modeling, identification and feedforward control of multivariable hysteresis by combining Bouc-Wen equations and the inverse multiplicative structure.. 2014 American Control Conference, ACC, Jan 2014, United States. pp.4771-4777. hal-01005451

HAL Id: hal-01005451

<https://hal.science/hal-01005451>

Submitted on 12 Jun 2014

HAL is a multi-disciplinary open access archive for the deposit and dissemination of scientific research documents, whether they are published or not. The documents may come from teaching and research institutions in France or abroad, or from public or private research centers.

L'archive ouverte pluridisciplinaire **HAL**, est destinée au dépôt et à la diffusion de documents scientifiques de niveau recherche, publiés ou non, émanant des établissements d'enseignement et de recherche français ou étrangers, des laboratoires publics ou privés.

Modeling, identification and feedforward control of multivariable hysteresis by combining Bouc-Wen equations and the inverse multiplicative structure

Didace HABINEZA, *Student Member, IEEE*,

Micky RAKOTONDRABE, *Member, IEEE* and Yann Le GORREC, *Member, IEEE*

Abstract—This paper deals with the modeling, identification and feedforward control of hysteresis found in multi-degrees of freedom (DOF) piezoelectric actuators. One main characteristic of the considered hysteresis behavior is the strong couplings. To express such multivariable hysteresis, we propose to extend the previous Bouc-Wen hysteresis monovariable model used for 1-DOF actuators. Then we propose to combine the resulting multivariable model with the inverse multiplicative structure in order to derive a multivariable compensator that suppresses the direct and the coupling hysteresis. Experimental tests on a piezotube scanner demonstrate the efficiency of the proposed approach.

I. INTRODUCTION

Piezoelectric based actuators are widely used in micro-nano positioning applications thanks to the high resolution, high bandwidth and high stiffness they can offer. However, the accuracy of their operation is compromised by hysteresis non-linearities [1]. Feedback control can be used to remove the hysteresis effects but, in some applications such as precise positioning, micromanipulation and microassembly, there is a lack of usable displacements sensors for that. Indeed, embeddable sensors (strain gage...) do not possess the required performances while performant sensors (optical sensors...) are very expensive and are bulky [2]. As an alternative to feedback control, feedforward control techniques have therefore been raised.

The most used feedforward hysteresis compensation approach is the model-based compensation, where hysteresis is first modelled. The calculated model is afterwards inverted and put in cascade with the actuator, in order to have a global linear system. Another approach is charge control based compensation where, instead of controlling the actuator by the voltage, the actuator displacement is controlled by the charge provided by an electronic circuit [3].

The most used model-based hysteresis models are Preisach and Prandtl-Ishlinskii. They can provide a very high accuracy thanks to the superposition of many elementary hysteresis operators (hysterons) [4][5][11][12]. However, their implementation can become complex if the number of the hysterons is very high. Furthermore, they are not easy to handle for structural analysis or synthesis (stability...). Finally, when

the system to be controlled has multiple degrees of freedom (multi-DOF), the number of parameters to be identified with these models increases exponentially as well as the number of hysterons, leading to a very complex calculation and implementation of the compensator. Contrary to that, the Bouc-Wen hysteresis model, which is based on a set of two equations, can offer a simplicity for handling, structural analysis/synthesis and for implementation. As it only uses four parameters, employing this to multi-DOF actuators may be of interest in term of simplicity, calculation and implementation.

In [6] hysteresis in multi-DOF systems is studied but feedback control techniques were used to remove the hysteresis. In [7][8][9][10] model-based control is used but it has been combined with feedback to suppress the hysteresis. In addition, couplings and the expected displacements are considered separately.

In this paper, we present the feedforward (open-loop) control of hysteresis in multi-DOF piezoactuators by considering the direct and the couplings between the axis. Based on the Bouc-Wen model used previously for mono-axis actuators, we give an extension to consider multivariable hysteresis. Then, we propose an identification procedure of the parameters and a multivariable compensator to eliminate the hysteresis behaviour and to suppress the couplings between the axis. Finally, experiments on a real system validate the efficiency of the proposed technique.

The paper is organized as follows. In section-II, we remind the monovariable Bouc-Wen model and we extend it to multivariable Bouc-Wen hysteresis model. In section-III, a procedure to identify the parameters of the proposed multivariable Bouc-Wen hysteresis model is proposed. Section-IV is devoted to the synthesis of a multivariable compensator for the hysteresis. Finally, section-V presents the experiments carried out with a multi-DOF piezoelectric actuator (piezotube).

II. MULTIVARIABLE BOUC-WEN HYSTERESIS MODELING

A. Remind of the monovariable Bouc-Wen modeling

Bouc-Wen model of hysteresis has been used in [13] (under equations (1)) as a relation between a mechanical excitation F , an output displacement y and a state variable h in nonlinear vibrational analysis. The parameters A , B and Γ govern the shape of the hysteresis while the power m affects the smoothness of the transition from elastic to

FEMTO-ST Institute, AS2M department, Université de Franche-Comté/CNRS/ENSM/UTBM, 25000 Besançon, France.

Didace Habineza: didace.habineza@femto-st.fr

Micky Rakotondrabe: mrakoton@femto-st.fr

Yann Le Gorrec: legorrec@femto-st.fr

plastic response. When the hysteresis is null, i.e. the internal variable h does not evolve, the Bouc-Wen model becomes a linear relation: $y = kF$ where k is the static gain. The influence (effect) of the different parameters is detailed in [14][15].

$$\begin{cases} y = kF - h \\ \dot{h} = A\dot{F} - B|\dot{F}|h|\dot{h}|^{m-1} - \Gamma\dot{F}|h|^m \end{cases} \quad (1)$$

For piezoelectric actuators where the driving signal is the voltage, the mechanical excitation F is replaced by input U . In addition, for piezoelectric based actuators, m can be assumed to be equal to 1 due to their elastic structure [13]. Consequently, the static Bouc-Wen model adapted to piezoactuators is described by equation (2) where d_p represents the piezoelectric coefficient, U the input voltage and y , the actuator deflection [1]. figure-1a depicts the block diagram of this Bouc-Wen model.

$$\begin{cases} y(t) = d_p U(t) - h(t) \\ \dot{h}(t) = A\dot{U}(t) - B|\dot{U}(t)|h(t) - \Gamma\dot{U}(t)|h(t)| \end{cases}, \quad \begin{aligned} y(t_0) &= y_0 \\ h(t_0) &= h_0 \end{aligned} \quad (2)$$

The previous Bouc-Wen expression can be reduced to (3) by writing $h = H(U)$ where $H(U)$ is a nonlinear operator characterized by the second equation of (2). The writing proposed in equation (3) is easier to handle when synthesizing a feedforward hysteresis compensator [1].

$$y = d_p U - H(U) \quad (3)$$

B. Extension to multivariable modeling

The existing Bouc-Wen model as described by equation (2) is used for monovariable hysteresis modeling and compensation. This cannot be used to model and then to calculate a compensator for actuators having multiple degrees of freedom. In this section, we propose to extend this monovariable model into multivariable Bouc-Wen hysteresis model with n inputs and n outputs. The corresponding diagram is represented in figure-1b where an input vector $\mathbf{U} = (U_1 \ U_2 \ \dots \ U_n)^T$ and an output vector $\mathbf{y} = (y_1 \ y_2 \ \dots \ y_n)^T$ are used.

To perform, let the following tensorial expression be the extension of the monovariable model of (2):

$$\underbrace{\begin{pmatrix} y_1 \\ y_2 \\ \vdots \\ y_n \end{pmatrix}}_{\mathbf{y}} = \underbrace{\begin{pmatrix} D_{11} & D_{12} & \dots & D_{1n} \\ D_{21} & D_{22} & \dots & D_{2n} \\ \vdots & \vdots & & \vdots \\ D_{n1} & D_{n2} & \dots & D_{nn} \end{pmatrix}}_{D_p} \underbrace{\begin{pmatrix} U_1 \\ U_2 \\ \vdots \\ U_n \end{pmatrix}}_{\mathbf{U}} - \underbrace{\begin{pmatrix} h_1 \\ h_2 \\ \vdots \\ h_n \end{pmatrix}}_{\mathbf{h}} \quad (4)$$

$$\begin{aligned} \underbrace{\begin{pmatrix} \dot{h}_1 \\ \dot{h}_2 \\ \vdots \\ \dot{h}_n \end{pmatrix}}_{\dot{\mathbf{h}}} &= \underbrace{\begin{pmatrix} A_{11} & A_{12} & \dots & A_{1n} \\ A_{21} & A_{22} & \dots & A_{2n} \\ \vdots & \vdots & & \vdots \\ A_{n1} & A_{n2} & \dots & A_{nn} \end{pmatrix}}_A \underbrace{\begin{pmatrix} \dot{U}_1 \\ \dot{U}_2 \\ \vdots \\ \dot{U}_n \end{pmatrix}}_{\dot{\mathbf{U}}} \\ &- \underbrace{\begin{pmatrix} B_{11} & B_{12} & \dots & B_{1n} \\ B_{21} & B_{22} & \dots & B_{2n} \\ \vdots & \vdots & & \vdots \\ B_{n1} & B_{n2} & \dots & B_{nn} \end{pmatrix}}_B \underbrace{\begin{pmatrix} |\dot{U}_1| & & & 0 \\ & |\dot{U}_2| & & \\ & & \ddots & \\ 0 & & & |\dot{U}_n| \end{pmatrix}}_{diag(|\dot{\mathbf{U}}|)} \underbrace{\begin{pmatrix} h_1 \\ h_2 \\ \vdots \\ h_n \end{pmatrix}}_{\mathbf{h}} \\ &- \underbrace{\begin{pmatrix} \Gamma_{11} & \Gamma_{12} & \dots & \Gamma_{1n} \\ \Gamma_{21} & \Gamma_{22} & \dots & \Gamma_{2n} \\ \vdots & \vdots & & \vdots \\ \Gamma_{n1} & \Gamma_{n2} & \dots & \Gamma_{nn} \end{pmatrix}}_{\Gamma} \underbrace{\begin{pmatrix} \dot{U}_1 & & & 0 \\ & \dot{U}_2 & & \\ & & \ddots & \\ 0 & & & \dot{U}_n \end{pmatrix}}_{diag(\dot{\mathbf{U}})} \underbrace{\begin{pmatrix} |h_1| \\ |h_2| \\ \vdots \\ |h_n| \end{pmatrix}}_{|\mathbf{h}|} \end{aligned} \quad (5)$$

i.e.

$$\begin{cases} y = D_p U - h \\ \dot{h} = A\dot{U} - Bdiag(|\dot{\mathbf{U}}|)h - \Gamma diag(\dot{\mathbf{U}})|h| \end{cases} \quad (6)$$

where $\mathbf{h} \in \mathbb{R}^n$ is a state vector and $A \in \mathbb{R}^{n \times n}$, $B \in \mathbb{R}^{n \times n}$ and $\Gamma \in \mathbb{R}^{n \times n}$ are the matricial parameters of the multivariable Bouc-Wen hysteresis model. In the next section, we propose a method to identify these parameters from experimental data.

III. IDENTIFICATION OF THE MULTIVARIABLE BOUC-WEN HYSTERESIS MODEL

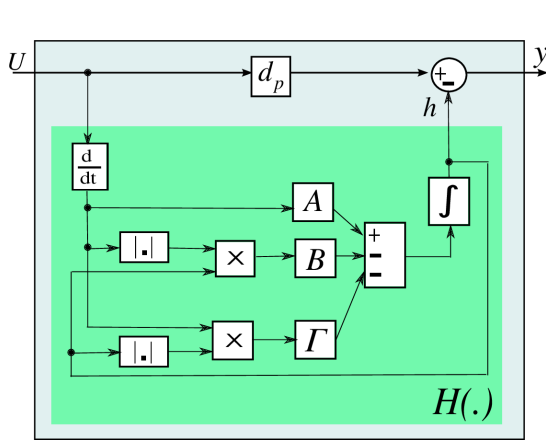
Equations (4) and (5) can be developed and written as:

$$\begin{cases} y_i = \left(\sum_{j=1}^n D_{ij} U_j \right) - h_i \\ \dot{h}_i = \sum_{j=1}^n A_{ij} \dot{U}_j - \sum_{j=1}^n B_{ij} |\dot{U}_j| h_j - \sum_{j=1}^n \Gamma_{ij} \dot{U}_j |h_j| \end{cases} \quad (7)$$

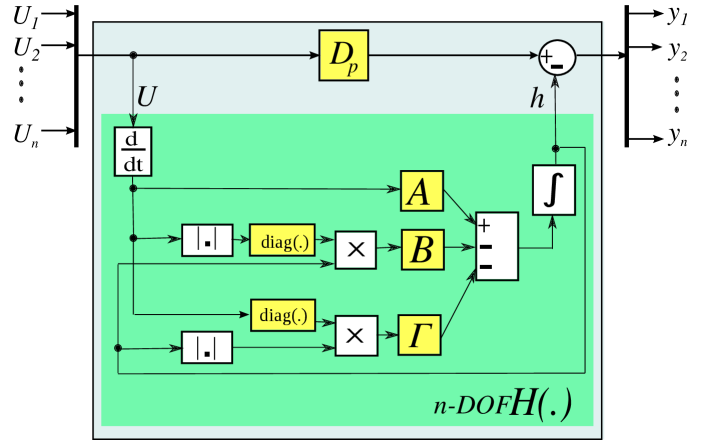
The parameters to be identified are D_{ij} , A_{ij} , B_{ij} and Γ_{ij} ($1 \leq i, j \leq n$) which are respectively the elements of the matrices D_p , A , B and Γ of equation (5). The subscript i denotes the considered output inside the vector \mathbf{y} , while j the considered input inside the vector \mathbf{U} . We notice that when $i = j$, we have the direct hysteresis and when $i \neq j$, we have the coupling hysteresis.

From the second equation of (7), we remark that all signals \dot{h}_i ($1 \leq i \leq n$) do not depend on h_i but on h_j (with j the subscript denoting the applied U). This means that for each applied voltage U_j ($1 \leq j \leq n$), all the outputs y_i ($1 \leq i \leq n$) which, naturally, depends on h_i also depends on h_j . So, the identification procedure follows the following steps:

Step 1 (experimental characterization): Apply a repetitive (sinusoidal or triangular) voltage input U_j (starting by $j = 1$) to the system and leave all the remaining inputs (i.e. all U_k with $k \neq j$ and $1 \leq k \leq n$) equal to zero. Capture all



(a) Diagram of 1-DOF Bouc-Wen hysteresis model.



(b) Diagram of n-DOF Bouc-Wen hysteresis model.

Fig. 1: 1-DOF and n-DOF Bouc-Wen model implementation.

the hysteresis curves (U_j, y_i) which, from equation (7), are derived as follows:

$$\begin{cases} y_i = D_{ij}U_j - h_i \\ \dot{h}_i = A_{ij}\dot{U}_j - B_{ij}|\dot{U}_j|h_j - \Gamma_{ij}\dot{U}_j|h_j| \end{cases} \quad (8)$$

Step 2 (identification of the direct hysteresis parameters): Identify, first, the parameters D_{jj} , A_{jj} , B_{jj} and Γ_{jj} from the direct hysteresis (U_j, y_i) (with $i = j$). This is done from equations:

$$\begin{cases} y_j = D_{jj}U_j - h_j \\ \dot{h}_j = A_{jj}\dot{U}_j - B_{jj}|\dot{U}_j|h_j - \Gamma_{jj}\dot{U}_j|h_j| \end{cases} \quad (9)$$

Step 3 (identification of the coupling hysteresis parameters): Then, identify the parameters D_{ij} , A_{ij} , B_{ij} and Γ_{ij} from the couplings hysteresis $((U_j, y_i)$ with $i \neq j$). This is done using equations (10):

$$\begin{cases} y_i = D_{ij}U_j - h_i \\ \dot{h}_i = A_{ij}\dot{U}_j - B_{ij}|\dot{U}_j|h_j - \Gamma_{ij}\dot{U}_j|h_j| \\ \dot{h}_j = A_{jj}\dot{U}_j - B_{jj}|\dot{U}_j|h_j - \Gamma_{jj}\dot{U}_j|h_j| \end{cases} \quad (10)$$

After that, repeat the previous three steps for $j = 2, 3, \dots, n$ to find the remaining parameters.

During **Step 2** and **Step 3**, the parameters are identified by using the least square Matlab optimization toolbox (lsqnonlin) designed to solve nonlinear data-fitting problems.

IV. FEEDFORWARD CONTROL OF THE MULTIVARIABLE BOUC-WEN HYSTERESIS MODEL

Assuming now that the parameters of the multivariable Bouc-Wen hysteresis model in (6) are identified, we present in this section a (multivariable) compensator for the hysteresis. The compensator is built in a way such that the feedforward controlled system as depicted in figure (2) satisfies the following condition:

$$y^d = y \quad (11)$$

where y^d (with $y^d = (y_1^d \ y_2^d \ \dots \ y_n^d)^T$) is the desired (reference) input vector.

The first equation of the multivariable model in (6) becomes therefore:

$$y^d = D_p U - h \quad (12)$$

From (12), the compensator is directly yielded as follows which has an inverse multiplicative structure:

$$U = D_p^{-1}(y^d + h) \quad (13)$$

where the control voltage U is the output of the compensator and the desired displacement y^d is its input. It is worth to notice that this compensator exists and is implementable because D_p is invertible. Indeed, when designing a multi-DOF actuators, the first natural expectation is that the input control U_i influence the output displacement y_i : in other words, the direct transfers D_{ii} are non-null. This means that the diagonal of the matrix D_p is non-null and therefore it is invertible. A case that may renders this matrix non-invertible is when the couplings annihilate some direct transfers. However this case is impossible or very rare for real processes.

In details, the compensator in equation (13) is written as in (14) while the simplified diagram for the multivariable hysteresis compensator with the proposed approach is represented in figure (2).

$$\underbrace{\begin{pmatrix} U_1 \\ U_2 \\ \vdots \\ U_n \end{pmatrix}}_U = \underbrace{\begin{pmatrix} D_{11} & D_{12} & \cdots & D_{1n} \\ D_{21} & D_{22} & \cdots & D_{2n} \\ \vdots & \vdots & \ddots & \vdots \\ D_{n1} & D_{n2} & \cdots & D_{nn} \end{pmatrix}^{-1}}_{D_p^{-1}} \underbrace{\begin{pmatrix} y_1^d + h_1 \\ y_2^d + h_2 \\ \vdots \\ y_n^d + h_n \end{pmatrix}}_{y^d + h} \quad (14)$$

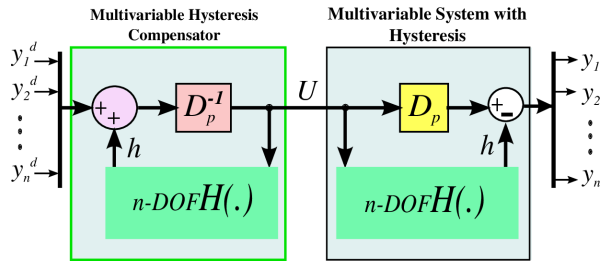


Fig. 2: n-DOF hysteresis compensator diagram.

The proposed approach is devoted to multi-DOF actuators. Another advantage is that there is no additional calculation to derive the compensator, except the inversion of D_p . As soon as the model is identified, the compensator is derived thanks to the inverse multiplicative structure.

V. EXPERIMENTAL RESULTS AND DISCUSSIONS

A. Experimental setup

The actuator used for the experiments is a PT230.94 piezotube scanner (from *PiCeraMic* company) that is often used in atomic force microscopy (AFM). This is an actuator designed to provide deflections along with three directions (X, Y and Z). The actuator is made up of PZT material (lead zirconate titanate), four external electrodes (+x, -x, +y and -y), and an inside electrode for ground (see figure (3)). $+U$ and $-U$ voltages can be applied on +x and -x electrodes (+y and -y respectively) to obtain tube deflections along the X direction (Y direction). Axial deformation (extension or elongation along the Z direction) is obtained by applying simultaneously $+U$ on the four external electrodes.

As the PT230.94 operating voltage range is $\pm 250V$, a high voltage amplifier is needed to amplify the control voltage. The tube deflections are measured by using optical displacement sensors (KC2420 from *Keyence* company). The sensors are set to have a resolution of $50nm$, an accuracy of $200nm$ and a bandwidth in excess of $1500kHz$. The sensors and the amplifier are connected to the computer through a 1103-dSPACE board (Figure (4)).

Due to the tubular shape of the actuator, it does not allow linear measurement with the optical displacement sensors. For this reason, we placed a small cube on the top of the piezotube with perpendicular sides pointing towards the sensors. Also, in the sequel, we are interested to the hysteresis behavior along the X and the Y axis and to their control. Accounting the general case where we are face to couplings, we can consider a bi-variable system with inputs U_x and U_y and with outputs X and Y .

B. System characterization, modeling and identification

This section is devoted to the characterization and modeling of the piezotube and the parameters identification.

• Multivariable Hysteresis Characterization:

We apply first a sine voltage U_x with an amplitude of $200V$ and a frequency of $0.1Hz$ to the x electrodes

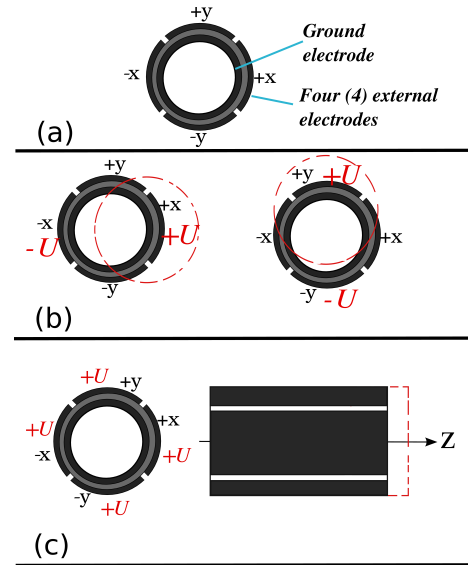


Fig. 3: (a) Top view showing the tube with its five electrodes (four external and one ground electrodes), (b) the tube bending in X and Y directions, (c) side view of the tube and its elongation in Z direction.

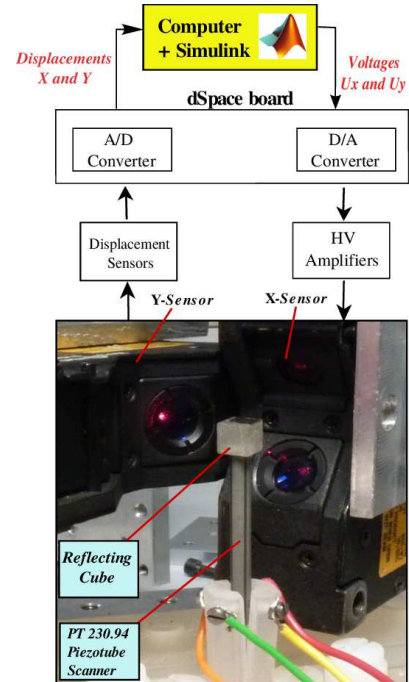


Fig. 4: Experimental setup description.

(+x and -x) and we let U_y be zero. The corresponding displacements X and Y are pictured respectively in figure (5 - (a) and (c)). Figure (5 - (a)) corresponds to the direct hysteresis along X axis while Figure (5 - (c)) corresponds to the coupling along Y axis due to U_x .

Then, U_x is set equal to zero and we apply the same sine voltage but to the y electrodes (+y and -y). The captured

deflections X and Y are represented in figure (5 - (b) and (d)). Figure (5 - (b)) corresponds to the coupling hysteresis along X axis due to U_y while Figure (5 - (d)) corresponds to the direct hysteresis along Y axis.

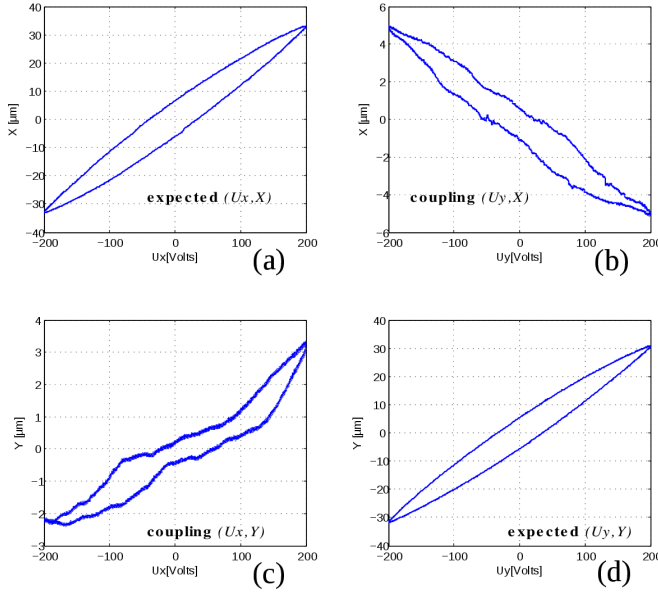


Fig. 5: Hysteresis Characterization: (a) and (c) represent X and Y displacements when only U_x is applied ($U_y = 0$), and (b) and (d) when only U_y is applied ($U_x = 0$). (a) and (d) represent the direct hysteresis, and (b) and (c) represent the couplings.

Notice that the chosen frequency ($0.1Hz$) used for the characterization and identification corresponds to the operational frequency when controlling the system.

- **Bouc-Wen parameters Identification and Validation:** This is done by following the steps discussed in section III. After obtaining the experimental hysteresis curves, we have identified the parameters of the multivariable Bouc-Wen model that fits with the experimental data by following these steps. The identified parameters are presented in table (I).

TABLE I: 2-DOF multivariable Hysteresis Bouc-Wen model parameters

	$U_x X$	$U_x Y$	$U_y X$	$U_y Y$
d_p	0.2042	0.0131	-0.0264	0.1930
A	0.0857	0.0032	-0.0086	0.0780
B	0.0072	0.0008	-0.0012	0.0100
Γ	0.0023	-0.0003	-0.0003	-0.0008

We mention that the model parameters are identified only from the external hysteresis loops, i.e from the hysteresis loops captured when the input voltage amplitude is in its maximal operating range ($\pm 200V$). Figures (6 - (a) to (d)) picture the comparison between the experimental hysteresis and the simulation of the identified model.

To validate the identified model, experiments and model simulation with lower input control voltages have also been

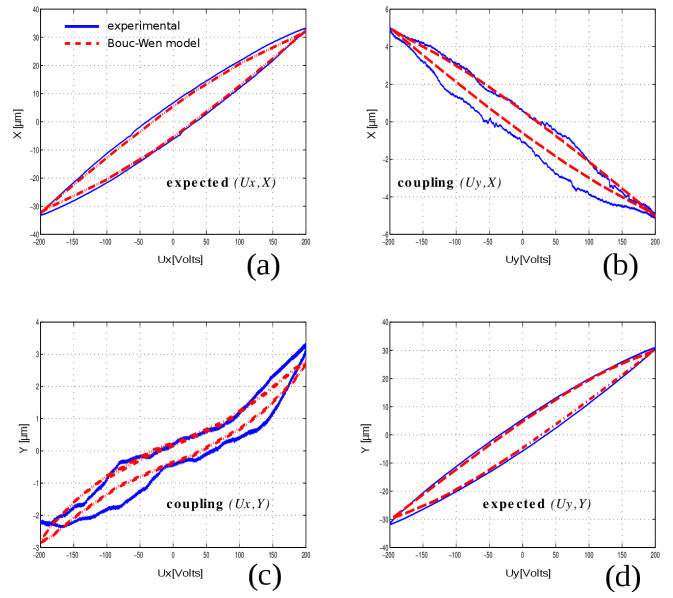


Fig. 6: Experimental curves and the simulation of the identified 2-DOF Bouc-Wen model.

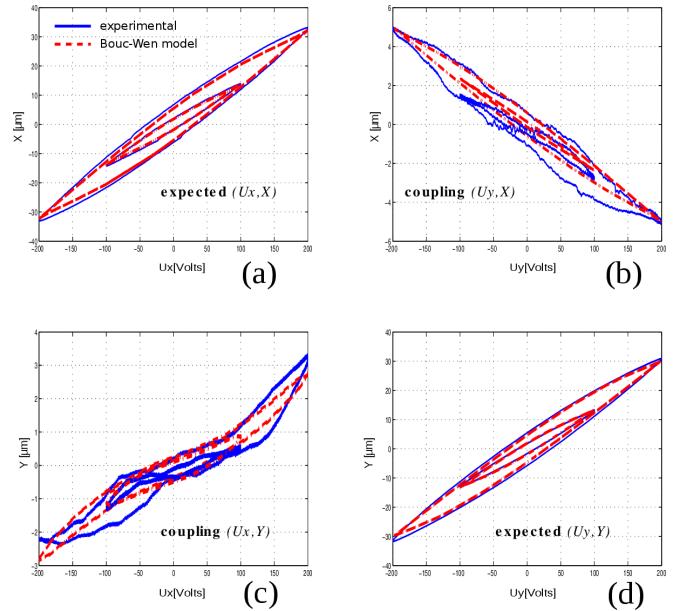


Fig. 7: Model validation: experimental curves and the simulation of the identified 2-DoF Bouc-Wen model with internal hysteresis loops (input voltages $\pm 100V$).

carried out. In figure (7), hysteresis with the external loops and hysteresis obtained with $\pm 100V$ input voltage are plotted.

The comparison in figures (6) and (7) shows the good convenience of the identified model. We remark however that the model of the couplings presents slight difference relative to the experiments. This is due to the fact that Bouc-Wen model only captures symmetric hysteresis.

C. Hysteresis compensation and experimental results

After the model identification and validation, we have implemented in Simulink-Matlab software the hysteresis compensator of figure (2). The compensator is built by using the parameters identified in section V-B. The actuator deflections, when controlled, with respect to the desired input commands, are represented in figure (8).

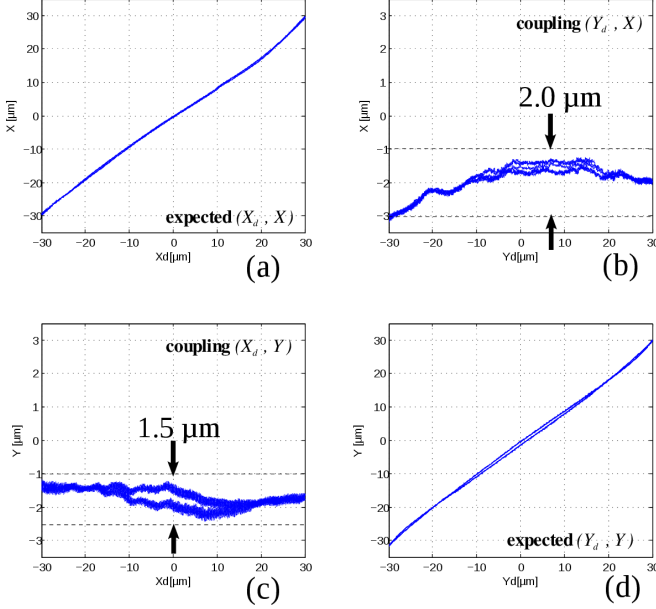


Fig. 8: Tube deflections after compensation. X_d and Y_d are applied separately. (a) and (d) show the expected deflections, and (b) and (c), the system couplings after compensation.

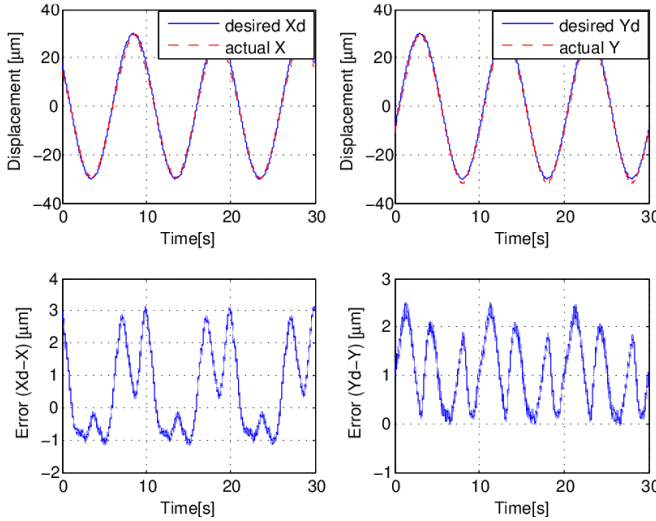


Fig. 9: Evaluation of tracking error with sinusoidal inputs, for expected deflections. X_d and Y_d are applied separately.

Comparing the initial hysteresis figures (5) with the results in (8) obtained with the compensator, we can clearly see that

the proposed compensator has almost suppressed hysteresis and reduced considerably the coupling amplitudes.

Figure (9) shows the tracking of sine input references X_d and Y_d , for expected deflections. It can be seen that, with the proposed compensator, the tracking error is less than $3 \mu m$ along X and $2.5 \mu m$ along Y axis.

We conclude from these figures that the input-output map between the desired displacements and the real output displacements reaches the expected linear behavior with unitary gain. Furthermore, the couplings are reduced to less than 3.3% of the amplitude of the desired displacements: less than $2 \mu m$ of coupling for $60 \mu m$ of desired displacements.

D. Complex trajectories tracking

In this subsection, we use a complex trajectory to the controlled piezotube. This has been done by tracking a circle with a radius of $20 \mu m$ in X - Y plane. Figure (10) pictures the results obtained with compensator and without compensator (scaled for the comparison). From this figure, we notice the improvement of the circular contouring when using the hysteresis compensator, i.e. the shape of the circle more regular. In addition, the accuracy is improved thanks to the hysteresis compensator.

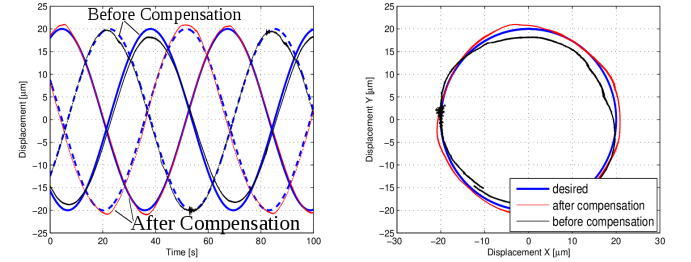


Fig. 10: Comparison between compensated and uncompensated system responses, by tracking a Circular Contour.

VI. CONCLUSIONS

In this paper, we presented the characterization, modeling, identification and feedforward compensation of hysteresis in multi-DOF piezoactuators. First, we proposed to model the multivariable hysteresis by extending the existing monovariable hysteresis into matricial model. The model permitted to account not only the hysteresis nonlinearities but also the couplings between the axis. Then, an appropriate identification procedure was proposed. The compensation is based on the combination of the yielded multivariable model and the inverse multiplicative structure. Two major advantages of the proposed compensator are its existence ensured and the fact that no additional calculation is required to derive it. As soon as the model is identified, the compensator is derived. Experimental tests with a piezoelectric tube (piezotube) working on 2-DOF have been carried out. The experiments, performed with classical signals and with more complex trajectory (circular), demonstrated the efficiency of the proposed modeling, identification and compensation techniques.

ACKNOWLEDGMENT

This work is supported by the national ANR-JCJC C-MUMS-project (National young investigator project ANR-12-JS03007.01: Control of Multivariable Piezoelectric Microsystems with Minimization of Sensors). A part of this work has also been supported by the national ANR-Emergence MYMESYS-project (ANR-11-EMMA-006: High Performances Embedded Measurement Systems for multiDegrees of Freedom Microsystems).

REFERENCES

- [1] Rakotondrabe, Micky, "Bouc-Wen modeling and inverse multiplicative structure to compensate hysteresis nonlinearity in piezoelectric actuators", *IEEE Transactions on Automation Science and Engineering*, pp.428-431 Vol.8, 2011
- [2] Devasia, Santosh and Eleftheriou, Evangelos and Moheimani, SO Reza, "A survey of Control Issues in Nanopositioning", *IEEE Transactions on Control Systems Technology*, pp.802-823 Vol.15, 2007
- [3] Clayton, GM and Tien, S and Fleming, AJ and Moheimani, SOR and Devasia, S, "Hysteresis and vibration compensation in piezoelectric actuators by integrating charge control and inverse feedforward", *4th IFAC Symp. Mechatron. Syst., Heidelberg, Germany*, 2006
- [4] Kuhnien, Klaus and Janocha, Hartmut, "Inverse feedforward controller for complex hysteretic nonlinearities in smart-material systems", *Control Intelligent Systems*, pp.74-83 Vol.29, 2001
- [5] R. V. Iyer, X. Tan, P. S. Krishnaprasad, "Approximate inversion of the Preisach hysteresis operator with application to control of smart actuators", *IEEE Transactions on Automatic Control*, vol. 50, no. 6, pp. 798-810, 2005
- [6] Merry, Roel and Uyanik, Mustafa and van de Molengraft, René and Koops, Richard and van Veghel, Marijn and Steinbuch, Maarten, "Identification, control and hysteresis compensation of a 3 DOF metrological AFM", *Asian Journal of Control*, pp.130-143 Vol.11, 2009
- [7] Yong, Yuen Kuan and Aphale, Sumeet S and Moheimani, SO Reza, "Design, identification, and control of a flexure-based XY stage for fast nanoscale positioning", *IEEE Transactions on Nanotechnology*, pp.46 Vol.8, 2009
- [8] Rakotondrabe, Micky and Agnus, Joël and Lutz, Philippe, "Feedforward and IMC-feedback control of a nonlinear 2-DOF piezoactuator dedicated to automated tasks", *IEEE Conference on Automation Science and Engineering*, pp.393-398, 2011
- [9] Micky Rakotondrabe and Kanty Rabenorosoa and Joël Agnus and Nicolas Chaillet, "Robust Feedforward-Feedback Control of a Nonlinear and Oscillating 2-DOF Piezocantilever", *IEEE T. Automation Science and Engineering*, pp.506-519 Vol.8, 2011
- [10] Xu, Qingsong and Li, Yangmin, "Dahl model-based hysteresis compensation and precise positioning control of an XY parallel micromanipulator with piezoelectric actuation", *Journal of dynamic systems, measurement, and control*, pp.041011 Vol.132, 2010
- [11] Al Janaideh, Mohammad and Su, Chun-Yi and Rakheja, Subhash, "Compensation of rate-dependent hysteresis nonlinearities in a piezo micro-positioning stage", *International Conference on Robotics and Automation (ICRA)*, pp.512-517, 2010
- [12] Ang, Wei Tech and Khosla, Pradeep K and Riviere, Cameron N, "Feedforward controller with inverse rate-dependent model for piezoelectric actuators in trajectory-tracking applications", *Transactions on Mechatronics, IEEE/ASME*, pp.134-142 Vol.12, 2007
- [13] Low, TS and Guo, W, "Modeling of a three-layer piezoelectric bimorph beam with hysteresis", *Journal of Microelectromechanical Systems*, pp.230-237 Vol.4, 1995
- [14] W.Schwanen, "Modelling and Identification of the dynamic behavior of a wire rope spring", Technische Universiteit Eindhoven, 2004
- [15] Sain, Patrick M and Sain, Michael K and Spencer, BF, "Models for Hysteresis and Application to Structural Control", *American Control Conference*, 1997
- [16] Rakotondrabe, Micky, "Classical Prandtl-Ishlinskii modeling and inverse multiplicative structure to compensate hysteresis in piezoactuators", *American Control Conference*, pp.1646-1651 Vol.10, 2012